Electronic Supplementary Material (ESI) for Chemical Communications.

Electronic Supplementary Information

A Cu_{12}-cluster-based metal-organic framework as a metastable intermediate in the formation of a layered copper phosphonate

Qian Teng, Ran Gao, Song-Song Bao,* Li-Min Zheng*

State Key Laboratory of Coordination Chemistry, School of Chemistry and Chemical Engineering, Collaborative Innovation Center of Advanced Microstructures, Nanjing University, Nanjing 210023, P. R. China

* Corresponding author. E-mail: lmzheng@nju.edu.cn, baososo@nju.edu.cn

EXPERIMENTAL SECTION

Materials and physical measurements. *R*-(1-phenylethylamino)methyl-phosphonic acid (*R*-pempH$_2$) was prepared according to methods reported in the literature.[1] All starting materials were analytical grade and obtained from commercial sources without further purification. Elemental analyses for C, H and N were carried out on a PE 240 C analyser. The FTIR spectra were recorded in the range of 400-4000 cm^{-1} by a Bruker Tensor 27 spectrometer. Thermogravimetric analyses (TGA) were carried out using METTLER TOLEDO TGA/DSC 1 instrument from 30 to 800 °C under a nitrogen atmosphere at a heating rate of 5 °C·min^{-1}. The powder X-ray diffraction (PXRD) patterns were collected using a Bruker D8 advance diffractometer. The circular dichroism (CD) spectra were recorded on a JASCO J-810 W spectropolarimeter at room temperature. The gas absorption and desorption isotherms were conducted by a BELSORP-Max adsorption analyzer. The UV/Vis spectra were measured on a Perkin Elmer Lambda 950 UV/VIS/NIR spectrometer using powder samples. The electrospray ionization mass spectrometry (ESI-MS) spectra were recorded using an LCQ fleet ESI-MS spectrometer (Thermo Scientific) in the positive and negative modes, and the isotopic distribution patterns of the observed species were simulated using the Xcalibur program.

Solid photothermal experiment. The Fotric 226s IR camera collected infrared photographs. An 808 nm light was generated through an infrared diode laser generator (MW-GX-808/5W from Changchun LASER Optoelectronics Tech Co, Ltd.), and the spot area is 1 cm^2. The sample was made into 7 mm^2 circular slice on 2.0 × 2.0 cm^2 glass sheets, and the distance between the laser lamp and the sample was changed to make the spot completely coincide with the sample.

Synthesis of [Cu$_{24}$(OH)$_{20}$(*R*-pempH)$_8$(SO$_4$)$_{10}$(H$_2$O)$_{10.5}$]·35H$_2$O (1). *R*-pempH$_2$ (11 mg, 0.05 mmol) was added in 3 mL deionized water in a 20 mL glass vial. After heating at 90 °C for 3 hours, a clear solution was obtained because of the dissolution of ligand. Then 100 μL imidazole (4 M) and 3 mL MeOH were added. After the solution was mixed uniformly, CuSO$_4$·5H$_2$O (75 mg, 0.29 mmol) was added and the glass vial was sealed. The mixture was placed at 90 °C for 3 hours, green octahedral block crystals of **1** were obtained. Yield: 9 mg, 37 % (based on *R*-pempH$_2$). Element analysis (EA) calcd (%) for C$_{72}$H$_{215}$Cu$_{24}$O$_{129.5}$P$_8$S$_{10}$N$_8$ (**1·35H$_2$O**): C, 16.14; H, 4.04; N, 2.09 %; found: C, 16.56; H, 3.93; N, 2.58 %. IR (KBr, cm^{-1}): 3070(w), 3285(m), 2986(w), 2806(w), 2522(w), 1623(w), 1504(w), 1453(w), 1378(m), 1283(w), 1151(w), 1113(m), 999(w), 770(w), 696(m), 605(m), 552(w), 514(w), 482(w).

Synthesis of [Cu$_2$(OH)(*R*-pempH)(SO$_4$)(H$_2$O)]·0.5H$_2$O·0.5CH$_3$OH (2). Compound **2** was synthesized in the same manner as compound **1**, except that the reaction time was extended to 18 hours. Yield: 13 mg, 59 % (based on *R*-pempH$_2$). Element analysis (EA) calcd (%) for C$_{9.5}$H$_{19}$Cu$_2$NO$_{10}$PS: C, 22.94; H, 3.85; N, 2.82 %; found: C, 22.63; H, 3.90; N, 2.86 %. IR (KBr, cm^{-1}): 3648(w), 3525(m), 3374(w), 2938(w), 2873(w), 2787(w), 2626(w), 2560(w), 2428(m), 2367(w), 1642(w), 1458(m), 1387(w), 1351(w), 1277(m), 1169(m), 1094(w), 1055(w), 897(w), 800(s), 783(s), 749(w), 710(s), 642(w), 611(w), 556(m), 528(w), 488(w), 448(m).

Single crystal X-ray Crystallography. Suitable single crystals of **1** and **2** were mounted on a loop ring, and diffraction data were collected using a Bruker D8 diffractometer equipped with TXS (Mo-Kα radiation, λ = 0.71073 Å). The collected data were integrated using the Siemens SAINT program,[2] and adsorption corrections were applied. The structures were solved using the intrinsic phasing method and refined on F^2 using full-matrix least-squares with the SHELXTL software package.[3] All the non-hydrogen atoms were refined anisotropically, while hydrogen atoms bound to carbon atoms and oxygen atoms of hydroxide were refined isotropically in the riding mode. In crystal 1, hydrogen atoms in the water molecules were

located in a difference map, added geometrically, and isotropically refined with a riding model. In crystal 2, the lattice water molecules are severely disordered and treatable by SQUEEZE.[4] The total potential solvent accessible void volume and electron count are 6087 Å and 1470, respectively, corresponding to approximately 140 water molecules per unit cell (35 H_2O per Cu_{24} unit). The hydrogen atoms of the coordinating water molecules can not be found in the Fourier map, so they were not included. Disordered SO_4^{2-} anions were treated accordingly, while regions of low occupancy were not refined for anisotropy. CCDC for **1** (2330623) and **2** (2330624) contain the supplementary crystallographic data for this paper. These data can be obtained free of charge from the Cambridge Crystallographic Data Centre via www.ccdc.cam.ac.uk/data_request/cif.

Reference:

[1] X.-G. Liu, et al. Polymorphism in homochiral zinc phosphonates. *Inorg. Chem*., 2008, 47, 5525–5527.
[2] SAINT, version 8.40A, Program for Data Extraction and Reduction, Bruker Nano. Inc., 2019.
[3] SHELXT 2014/5, Sheldrick, 2014; SHELXL 2018/3, Sheldrick, 2018.
[4] A. L. Spek. PLATON SQUEEZE: a tool for the calculation of the disordered solvent contribution to the calculated structure factors. *Acta Cryst.* 2015, C71, 9–18.

Table S1 Crystal data and structure refinements for **1** and **2**

Compounds	**1**	**2**
Formula	$C_{72}H_{145}Cu_{24}O_{94.5}P_8S_{10}N_8$	$C_{9.5}H_{19}Cu_2NO_{10}PS$
M	4728.27	497.37
Crystal system	monoclinic	orthorhombic
Space group	*C*2	$P2_12_12_1$
a (Å)	32.3485(10)	7.0932(3)
b (Å)	19.7547(5)	7.3733(4)
c (Å)	32.5262(9)	31.2935(15)
α (°)	90	90
β (°)	112.6600(10)	90
γ (°)	90	90
V (Å^3)	19180.9(9)	1636.66(14)
Z	4	4
D_c (g cm^{-3})	1.637	2.018
μ (mm^{-1})	2.858	2.876
F (000)	9460.0	1008.0
R_{int}	0.0410	0.0344
GoF on F^2	1.044	1.079
R_1, wR_2[a] [$I > 2\sigma(I)$]	0.0452, 0.1220	0.0230, 0.0596
CCDC	2330623	2330624

$R_1 = \Sigma||F_o| - |F_c||/\Sigma|F_o|$, $wR_2 = [\Sigma w(F_o^2 - F_c^2)^2/\Sigma w(F_o^2)^2]^{1/2}$

Table S2. Selected bond lengths [Å] and bond angles [°] of **1**.

Cu1-O1	2.167(6)	Cu9-O11	2.373(6)	Cu17-O22	2.045(8)
Cu1-O4	2.133(6)	Cu9-O32	1.951(6)	Cu17-O39	1.941(7)
Cu1-O25	1.950(6)	Cu9-O33	1.923(6)	Cu17-O40	1.882(8)
Cu1-O26	1.908(6)	Cu9-O61	1.967(6)	Cu17-O70	1.996(9)
Cu1-O45	2.253(7)	Cu10-O6	2.009(6)	Cu18-O17	2.324(7)
Cu1-O49	2.121(7)	Cu10-O9	2.233(5)	Cu18-O22	1.991(7)
Cu2-O1	1.989(6)	Cu10-O28	1.913(6)	Cu18-O39	1.972(7)
Cu2-O7	2.251(6)	Cu10-O34	1.987(5)	Cu18-O41	1.887(8)
Cu2-O25	1.979(6)	Cu10-O65	2.005(6)	Cu18-O8W	1.999(8)
Cu2-O27	1.887(6)	Cu11-O6	2.233(6)	Cu19-O15	1.967(8)
Cu2-O1W	2.007(7)	Cu11-O12	1.975(6)	Cu19-O20	2.252(8)
Cu3-O4	2.004(6)	Cu11-O30	1.900(6)	Cu19-O37	1.893(9)
Cu3-O7	2.199(6)	Cu11-O34	1.955(6)	Cu19-O42	1.967(8)
Cu3-O25	1.979(6)	Cu11-O67	1.982(11)	Cu19-O77	2.074(9)
Cu3-O28	1.904(6)	Cu11-O11W	1.954(11)	Cu20-O15	2.214(8)
Cu3-O2W	2.044(7)	Cu12-O9	1.953(6)	Cu20-O23	1.993(8)
Cu4-O2	2.089(6)	Cu12-O12	2.422(6)	Cu20-O40	1.915(9)
Cu4-O5	2.088(6)	Cu12-O33	1.951(6)	Cu20-O42	1.941(9)
Cu4-O26	1.896(6)	Cu12-O34	2.015(6)	Cu20-O74	2.070(13)
Cu4-O29	1.955(6)	Cu12-O5W	1.989(7)	Cu21-O20	1.969(8)
Cu4-O64A	2.044(7)	Cu13-O13	2.139(9)	Cu21-O23	2.358(9)
Cu5-O5	2.197(6)	Cu13-O16	2.178(7)	Cu21-O42	1.997(9)
Cu5-O10	2.015(5)	Cu13-O35	1.958(7)	Cu21-O43	1.922(9)
Cu5-O29	1.963(6)	Cu13-O36	1.893(7)	Cu21-O9W	1.991(11)
Cu5-O30	1.896(6)	Cu13-O46	2.151(7)	Cu22-O18	1.994(8)
Cu5-O53	1.978(6)	Cu13-O50	2.219(7)	Cu22-O21	2.209(8)
Cu6-O2	2.328(6)	Cu14-O13	1.982(7)	Cu22-O38	1.922(7)
Cu6-O10	2.003(6)	Cu14-O19	2.237(7)	Cu22-O44	1.971(7)
Cu6-O29	1.937(6)	Cu14-O35	1.960(7)	Cu22-O79	2.008(8)
Cu6-O31	1.900(6)	Cu14-O37	1.916(9)	Cu22-O10W	2.508(11)
Cu6-O3W	2.006(7)	Cu14-O6W	2.030(9)	Cu23-O18	2.297(8)
Cu7-O3	2.004(6)	Cu15-O16	2.002(7)	Cu23-O24	1.997(8)
Cu7-O8	2.253(6)	Cu15-O19	2.237(7)	Cu23-O41	1.869(8)
Cu7-O27	1.904(6)	Cu15-O35	1.985(7)	Cu23-O44	1.947(7)
Cu7-O32	1.967(6)	Cu15-O38	1.916(7)	Cu23-O73	2.027(9)
Cu7-O57	2.028(7)	Cu15-O7W	2.056(8)	Cu24-O21	1.966(7)
Cu7-O4W	2.588(8)	Cu16-O14	2.129(8)	Cu24-O24	2.369(8)
Cu8-O3	2.298(6)	Cu16-O17	2.089(8)	Cu24-O43	1.890(8)
Cu8-O11	2.009(6)	Cu16-O36	1.883(6)	Cu24-O44	1.977(7)
Cu8-O31	1.894(6)	Cu16-O39	1.946(6)	Cu24-O83	2.030(2)
Cu8-O32	1.925(6)	Cu16-O85C	2.176(13)	Cu24-O83'	2.070(5)
Cu8-O55B	2.022(7)	Cu16-O85'C	2.060(2)	P1-O1	1.517(6)
Cu9-O8	1.963(6)	Cu17-O14	2.169(7)	P1-O2	1.507(6)

P1-O3	1.510(6)	P4-O10	1.546(6)	P6-O17	1.502(8)
P2-O4	1.518(6)	P4-O11	1.515(6)	P6-O18	1.524(8)
P2-O5	1.517(6)	P4-O12	1.518(6)	P7-O19	1.488(8)
P2-O6	1.508(7)	P5-O13	1.532(8)	P7-O20	1.509(9)
P3-O7	1.502(6)	P5-O14	1.507(8)	P7-O21	1.527(8)
P3-O8	1.522(6)	P5-O15	1.526(9)	P8-O22	1.526(8)
P3-O9	1.534(6)	P6-O16	1.528(7)	P8-O23	1.500(8)
O1-Cu1-O45	169.1(2)	O26-Cu4-O5	96.8(2)	P8-O24	1.495(8)
O4-Cu1-O1	92.2(2)	O26-Cu4-O29	179.4(3)	O32-Cu7-O3	83.8(2)
O4-Cu1-O45	87.0(2)	O26-Cu4-O64A	87.3(3)	O32-Cu7-O8	76.6(2)
O25-Cu1-O1	78.9(2)	O29-Cu4-O2	82.7(2)	O32-Cu7-O57	88.9(3)
O25-Cu1-O4	79.1(2)	O29-Cu4-O5	82.6(2)	O32-Cu7-O4W	96.1(2)
O25-Cu1-O45	90.2(2)	O29-Cu4-O64A	93.2(2)	O57-Cu7-O8	93.8(2)
O25-Cu1-O49	93.0(2)	O64A-Cu4-O2	127.5(3)	O57-Cu7-O4W	84.5(2)
O26-Cu1-O1	98.0(2)	O64A-Cu4-O5	129.3(3)	O11-Cu8-O3	98.2(2)
O26-Cu1-O4	97.5(3)	O10-Cu5-O5	95.7(2)	O11-Cu8-O55B	163.9(3)
O26-Cu1-O25	175.3(2)	O29-Cu5-O5	79.7(2)	O31-Cu8-O3	102.6(2)
O26-Cu1-O45	92.9(3)	O29-Cu5-O10	79.8(2)	O31-Cu8-O32	178.8(2)
O26-Cu1-O49	90.7(3)	O29-Cu5-O53	88.7(2)	O31-Cu8-O55B	89.0(3)
O49-Cu1-O1	92.7(2)	O30-Cu5-O5	106.0(2)	O32-Cu8-O3	77.2(2)
O49-Cu1-O4	169.8(3)	O30-Cu5-O10	93.4(3)	O32-Cu8-O11	85.2(2)
O49-Cu1-O45	86.6(3)	O30-Cu5-O29	171.6(3)	O32-Cu8-O55B	92.2(3)
O1-Cu2-O7	97.1(2)	O30-Cu5-O53	96.4(3)	O55B-Cu8-O3	96.7(3)
O1-Cu2-O1W	170.1(3)	O53-Cu5-O5	98.3(3)	O8-Cu9-O11	94.0(2)
O25-Cu2-O1	82.7(2)	O53-Cu5-O10	160.0(3)	O8-Cu9-O61	163.2(3)
O25-Cu2-O7	80.1(2)	O10-Cu6-O2	96.1(2)	O32-Cu9-O8	84.3(2)
O25-Cu2-O1W	90.9(3)	O10-Cu6-O3W	166.3(3)	O32-Cu9-O11	75.3(2)
O27-Cu2-O1	92.7(3)	O29-Cu6-O2	77.0(2)	O32-Cu9-O61	89.2(3)
O27-Cu2-O7	104.8(2)	O29-Cu6-O10	80.7(2)	O33-Cu9-O8	94.2(2)
O27-Cu2-O25	173.7(3)	O29-Cu6-O3W	91.6(3)	O33-Cu9-O11	100.4(2)
O27-Cu2-O1W	93.1(3)	O31-Cu6-O2	104.7(2)	O33-Cu9-O32	175.3(3)
O1W-Cu2-O7	89.2(3)	O31-Cu6-O10	93.6(2)	O33-Cu9-O61	93.4(3)
O4-Cu3-O7	98.8(2)	O31-Cu6-O29	174.5(3)	O61-Cu9-O11	99.3(2)
O4-Cu3-O2W	170.0(3)	O31-Cu6-O3W	93.6(3)	O6-Cu10-O9	89.4(2)
O25-Cu3-O4	81.7(3)	O3W-Cu6-O2	93.2(3)	O34-Cu10-O9	76.3(2)
O25-Cu3-O7	81.4(2)	O3-Cu7-O8	98.7(2)	O34-Cu10-O65	92.7(2)
O25-Cu3-O2W	92.9(3)	O3-Cu7-O57	163.6(3)	O28-Cu10-O6	93.1(3)
O28-Cu3-O4	93.3(3)	O3-Cu7-O4W	81.8(2)	O28-Cu10-O9	105.2(2)
O28-Cu3-O7	101.3(2)	O8-Cu7-O4W	172.5(2)	O28-Cu10-O34	176.7(3)
O28-Cu3-O25	174.7(3)	O27-Cu7-O3	93.6(3)	O28-Cu10-O65	90.2(3)
O28-Cu3-O2W	91.8(3)	O27-Cu7-O8	99.7(2)	O34-Cu10-O6	83.9(2)
O2W-Cu3-O7	88.6(3)	O27-Cu7-O32	175.0(3)	O65-Cu10-O6	175.5(3)
O2-Cu4-O5	102.2(2)	O27-Cu7-O57	94.7(3)	O65-Cu10-O9	92.7(2)
O26-Cu4-O2	97.3(3)	O27-Cu7-O4W	87.7(3)	O12-Cu11-O6	100.6(3)

O12-Cu11-O67	175.6(4)	O37-Cu14-O6W	96.8(4)	O15-Cu19-O77	170.2(4)
O30-Cu11-O6	102.1(2)	O6W-Cu14-O19	85.8(3)	O37-Cu19-O15	92.1(4)
O30-Cu11-O12	92.7(3)	O16-Cu15-O19	96.4(3)	O37-Cu19-O20	103.0(3)
O30-Cu11-O34	178.1(3)	O16-Cu15-O7W	170.8(3)	O37-Cu19-O42	175.4(4)
O30-Cu11-O67	89.3(4)	O35-Cu15-O16	83.0(3)	O37-Cu19-O77	94.6(4)
O30-Cu11-O11W	92.0(4)	O35-Cu15-O19	79.8(3)	O42-Cu19-O15	83.3(3)
O34-Cu11-O6	79.0(2)	O35-Cu15-O7W	89.5(3)	O42-Cu19-O20	77.7(3)
O34-Cu11-O12	85.6(2)	O38-Cu15-O16	93.3(3)	O42-Cu19-O77	89.9(4)
O34-Cu11-O67	92.4(3)	O38-Cu15-O19	102.2(3)	O77-Cu19-O20	91.3(3)
O34-Cu11-O11W	88.9(4)	O38-Cu15-O35	176.0(3)	O23-Cu20-O15	97.2(3)
O67-Cu11-O6	82.8(4)	O38-Cu15-O7W	94.0(3)	O23-Cu20-O74	177.6(5)
O11W-Cu11-O6	112.1(5)	O7W-Cu15-O19	87.3(3)	O40-Cu20-O15	101.6(3)
O11W-Cu11-O12	145.2(5)	O14-Cu16-O85C	156.8(4)	O40-Cu20-O23	95.1(3)
O9-Cu12-O12	91.9(2)	O17-Cu16-O14	104.6(3)	O40-Cu20-O42	178.8(3)
O9-Cu12-O33	91.7(2)	O17-Cu16-O85C	96.2(5)	O40-Cu20-O74	83.6(4)
O9-Cu12-O34	82.4(2)	O36-Cu16-O14	96.8(3)	O42-Cu20-O15	77.7(3)
O9-Cu12-O5W	173.7(3)	O36-Cu16-O17	98.5(3)	O42-Cu20-O23	84.0(3)
O33-Cu12-O12	106.6(2)	O36-Cu16-O39	177.4(3)	O42-Cu20-O74	97.3(4)
O33-Cu12-O34	174.1(2)	O36-Cu16-O85C	90.5(4)	O74-Cu20-O15	85.0(5)
O33-Cu12-O5W	93.2(3)	O36-Cu16-O85'C	89.5(6)	O20-Cu21-O23	94.8(3)
O34-Cu12-O12	73.3(2)	O39-Cu16-O14	82.4(3)	O20-Cu21-O42	83.5(3)
O5W-Cu12-O12	90.6(3)	O39-Cu16-O17	84.1(3)	O20-Cu21-O9W	171.7(4)
O5W-Cu12-O34	92.7(3)	O39-Cu16-O85C	89.4(4)	O42-Cu21-O23	73.9(3)
O13-Cu13-O16	92.0(3)	O39-Cu16-O85'C	88.3(6)	O42-Cu21-O9W	89.2(5)
O13-Cu13-O46	169.5(3)	O85'C-Cu16-O14	99.9(7)	O43-Cu21-O20	92.7(4)
O13-Cu13-O50	87.5(3)	O85'C-Cu16-O17	153.0(6)	O43-Cu21-O23	103.5(3)
O16-Cu13-O50	171.7(3)	O22-Cu17-O14	97.0(3)	O43-Cu21-O42	175.2(3)
O35-Cu13-O13	77.9(3)	O39-Cu17-O14	81.5(3)	O43-Cu21-O9W	94.7(5)
O35-Cu13-O16	79.2(3)	O39-Cu17-O22	80.4(3)	O9W-Cu21-O23	86.9(5)
O36-Cu13-O50	92.4(3)	O39-Cu17-O70	87.3(3)	O18-Cu22-O21	96.2(3)
O46-Cu13-O16	92.1(3)	O40-Cu17-O14	102.3(3)	O18-Cu22-O79	170.5(4)
O46-Cu13-O50	87.0(3)	O40-Cu17-O22	94.8(3)	O18-Cu22-O10W	82.4(4)
O35-Cu13-O46	93.4(3)	O40-Cu17-O39	174.3(3)	O38-Cu22-O79	88.6(3)
O35-Cu13-O50	92.7(3)	O40-Cu17-O70	95.9(4)	O38-Cu22-O10W	87.9(3)
O36-Cu13-O13	98.9(3)	O70-Cu17-O14	103.0(4)	O44-Cu22-O18	83.3(3)
O36-Cu13-O16	95.9(3)	O39-Cu18-O17	77.5(3)	O44-Cu22-O21	77.4(3)
O36-Cu13-O35	173.9(3)	O39-Cu18-O22	81.0(3)	O44-Cu22-O79	93.2(3)
O13-Cu14-O6W	168.9(4)	O39-Cu18-O8W	91.8(3)	O44-Cu22-O10W	91.5(3)
O35-Cu14-O13	81.7(3)	O41-Cu18-O17	103.3(3)	O79-Cu22-O21	91.6(3)
O35-Cu14-O19	80.3(3)	O41-Cu18-O22	93.3(3)	O79-Cu22-O10W	88.9(4)
O35-Cu14-O6W	88.0(4)	O41-Cu18-O39	174.3(3)	O24-Cu23-O18	97.5(3)
O37-Cu14-O13	93.3(4)	O41-Cu18-O8W	93.7(3)	O41-Cu23-O24	92.1(3)
O37-Cu14-O19	102.2(3)	O8W-Cu18-O17	94.4(3)	O41-Cu23-O44	177.5(3)
O37-Cu14-O35	174.7(3)	O22-Cu18-O8W	164.5(3)	O41-Cu23-O73	93.4(3)

O44-Cu23-O18	76.3(3)	O21-Cu24-O83	166.7(7)	O43-Cu24-O83'	97.5(1)
O44-Cu23-O24	86.0(3)	O21-Cu24-O83'	166.1(1)	O44-Cu24-O24	75.9(3)
O44-Cu23-O73	88.9(3)	O43-Cu24-O21	94.0(3)	O44-Cu24-O83	90.7(5)
O73-Cu23-O18	96.2(3)	O43-Cu24-O24	101.6(3)	O44-Cu24-O83'	85.6(1)
O21-Cu24-O24	91.6(3)	O43-Cu24-O44	176.2(3)	O83-Cu24-O24	98.4(5)
O21-Cu24-O44	83.2(3)	O43-Cu24-O83	92.6(5)	O83'-Cu24-O24	93.7(1)
Cu2-O1-Cu1	94.7(2)	Cu24-O21-Cu22	94.9(3)	Cu11-O34-Cu10	103.0(3)
Cu4-O2-Cu6	91.4(2)	Cu18-O22-Cu17	96.3(3)	Cu11-O34-Cu12	107.8(2)
Cu7-O3-Cu8	92.5(2)	Cu20-O23-Cu21	93.9(3)	Cu13-O35-Cu14	103.0(3)
Cu3-O4-Cu1	95.6(2)	Cu23-O24-Cu24	91.4(3)	Cu13-O35-Cu15	102.0(3)
Cu4-O5-Cu5	92.8(2)	Cu1-O25-Cu2	102.2(2)	Cu14-O35-Cu15	108.5(3)
Cu10-O6-Cu11	93.2(2)	Cu1-O25-Cu3	102.6(3)	Cu16-O36-Cu13	123.4(4)
Cu3-O7-Cu2	91.3(2)	Cu2-O25-Cu3	107.1(3)	Cu19-O37-Cu14	122.5(4)
Cu9-O8-Cu7	93.8(2)	Cu4-O26-Cu1	122.9(3)	Cu15-O38-Cu22	120.5(4)
Cu12-O9-Cu10	95.9(2)	Cu2-O27-Cu7	122.3(3)	Cu16-O39-Cu18	107.3(3)
Cu6-O10-Cu5	96.7(2)	Cu3-O28-Cu10	121.6(3)	Cu17-O39-Cu16	104.6(3)
Cu8-O11-Cu9	90.9(2)	Cu4-O29-Cu5	104.7(3)	Cu17-O39-Cu18	100.4(3)
Cu11-O12-Cu12	93.2(2)	Cu6-O29-Cu4	108.9(3)	Cu17-O40-Cu20	121.4(4)
Cu14-O13-Cu13	96.1(3)	Cu6-O29-Cu5	100.6(3)	Cu23-O41-Cu18	122.7(4)
Cu16-O14-Cu17	91.4(3)	Cu5-O30-Cu11	119.8(3)	Cu19-O42-Cu21	103.3(4)
Cu19-O15-Cu20	94.4(3)	Cu8-O31-Cu6	121.0(3)	Cu20-O42-Cu19	103.7(4)
Cu15-O16-Cu13	94.2(3)	Cu8-O32-Cu7	106.3(3)	Cu20-O42-Cu21	108.1(4)
Cu16-O17-Cu18	91.1(3)	Cu8-O32-Cu9	107.8(3)	Cu24-O43-Cu21	122.7(4)
Cu22-O18-Cu23	93.8(3)	Cu9-O32-Cu7	103.8(3)	Cu22-O44-Cu24	102.6(3)
Cu15-O19-Cu14	91.4(3)	Cu9-O33-Cu12	121.4(3)	Cu23-O44-Cu22	106.5(3)
Cu21-O20-Cu19	94.6(3)	Cu10-O34-Cu12	102.2(3)	Cu23-O44-Cu24	106.0(3)

Symmetry transformations used to generate equivalent atoms: A: -*x*+3/2, *y*-1/2, -*z*+2; B: -*x*+3/2, *y*+1/2, -*z*+2; C: -*x*+3/2, *y*+1/2, -*z*+1.

Table S3 Partial bond lengths [Å] and bond angles [°] of **2**.

Cu1-O1	1.954(3)	Cu2-O2D	1.933(3)	P1-O2	1.508(3)
Cu1-O3A	1.960(3)	Cu2-O3E	2.369(3)	P1-O3	1.515(3)
Cu1-O4	2.380(3)	Cu2-O5	1.977(3)	S1-O4	1.479(3)
Cu1-O7B	2.397(3)	Cu2-O8	2.022(3)	S1-O5	1.491(3)
Cu1-O8	1.966(3)	Cu2-O1W	1.950(7)	S1-O6	1.461(3)
Cu1-O8B	1.975(3)	Cu2-O1W'	1.965(15)	S1-O7	1.476(3)
Cu2-O1	2.435(3)	P1-O1	1.518(3)		
O1-Cu1-O3A	178.5(2)	O8B-Cu1-O7B	90.3(1)	O5-Cu2-O8	97.8(1)
O1-Cu1-O4	88.6(2)	O8-Cu1-O7B	90.5(1)	O8-Cu2-O1	71.8(1)
O1-Cu1-O7B	91.3(1)	O8-Cu1-O8B	179.1(4)	O8-Cu2-O3E	73.6(1)
O1-Cu1-O8B	95.2(1)	O2D-Cu2-O1	90.2(1)	O1W-Cu2-O1	117.9(3)
O1-Cu1-O8	84.4(1)	O2D-Cu2-O3E	93.5(1)	O1W-Cu2-O3E	96.8(3)
O3A-Cu1-O4	92.8(1)	O2D-Cu2-O5	177.0(2)	O1W-Cu2-O5	83.5(3)
O3A-Cu1-O7B	87.2(1)	O2D-Cu2-O8	83.8(1)	O1W-Cu2-O8	170.3(3)
O3A-Cu1-O8B	84.6(1)	O2D-Cu2-O1W	95.4(3)	O1W'-Cu2-O1	97.0(4)
O3A-Cu1-O8	95.8(1)	O2D-Cu2-O1W'	95.3(5)	O1W'-Cu2-O5	82.9(5)
O4-Cu1-O7B	178.7(1)	O3E-Cu2-O1	144.6(9)	O1W'-Cu2-O8	168.9(4)
O8-Cu1-O4	90.8(1)	O5-Cu2-O1	87.7(1)	Cu1-O1-Cu2	92.1(1)
O8B-Cu1-O4	88.3(1)	O5-Cu2-O3E	89.6(1)	Cu1B-O3-Cu2	92.7(1)
Cu1-O8-Cu1A	128.3(2)	Cu1-O8-Cu2	105.6(2)	Cu1A -O8-Cu2	103.8(1)

Symmetry transformations used to generate equivalent atoms: A: *x*+1/2, -*y*+3/2, -*z*+1; B: *x*-1/2, -*y*+3/2, -*z*+1; C: *x*-1/2, -*y*+1/2, -*z*+1; D: *x*+1/2, -*y*+1/2-*z*+1; E: *x*+1, *y*, *z*.

Table S4 Possible molecular fragments of the reaction solutions at 1h, 2h, and 3h (positive charge scan mode, m/z 400 - 2500).

positive charge scan mode (1h)		
Possible molecular fragments	Formula weight	The main spectral peak
$[Cu_3(OH)_3(SO_4)(H_2O)_5(CH_3OH)]^+$	459.8	459.3
$[Cu_3(OH)_2(pempH)(SO_4)(H_2O)(CH_3OH)]^+$	584.5	583.5
$[Cu_4(OH)_3(pempH)_2(SO_4)(H_2O)_3]^+$	883.69	883.25
$[Cu_5(OH)_2(pempH)(SO_4)_3(H_2O)_4(CH_3OH)]^+$	958.2	957.2
$[Cu_6(OH)_2(pempH)(SO_4)_4(H_2O)]^+$	1031.76	1031.29
$[Cu_6(OH)_3(pempH)_2(SO_4)_3(H_2O)_6]^+$	1254	1254.35
$[Cu_9(OH)_6(pempH)(SO_4)_5(H_2O)_2]^+$	1403.53	1403.38
$[Cu_6(OH)_3(pempH)_4(SO_4)_2(H_2O)_4]^+$	1552	1551.4
positive charge scan mode (2h)		
$[Cu_3(OH)_2(pempH)(SO_4)(H_2O)(CH_3OH)]^+$	584.5	583.5
$[Cu_3(OH)(pempH)_2(SO_4)]^+$	731.5	731.49
$[Cu_4(OH)_3(pempH)_2(SO_4)(H_2O)_3]^+$	883.69	883.25
$[Cu_5(OH)_2(pempH)(SO_4)_3(H_2O)_4(CH_3OH)]^+$	958.2	957.2
$[Cu_6(OH)_2(pempH)(SO_4)_4(H_2O)]^+$	1031.76	1031.29
$[Cu_6(OH)_3(pempH)_2(SO_4)_3(H_2O)_6]^+$	1254	1254.35
$[Cu_9(OH)_6(pempH)(SO_4)_5(H_2O)_2]^+$	1403.53	1403.38
$[Cu_6(OH)_3(pempH)_4(SO_4)_2(H_2O)_4]^+$	1552	1551.4
positive charge scan mode (3h)		
$[Cu_4(OH)_3(pempH)_2(SO_4)(H_2O)_3]^+$	883.69	883.25
$[Cu_5(OH)_2(pempH)(SO_4)_3(H_2O)_4(CH_3OH)]^+$	958.2	957.2
$[Cu_6(OH)_2(pempH)(SO_4)_4(H_2O)]^+$	1031.76	1031.29
$[Cu_6(OH)_3(pempH)_2(SO_4)_3(H_2O)_6]^+$	1254	1254.35
$[Cu_9(OH)_6(pempH)(SO_4)_5(H_2O)_2]^+$	1403.53	1403.38
$[Cu_6(OH)_3(pempH)_4(SO_4)_2(H_2O)_4]^+$	1552	1551.4

Table S5 Possible molecular fragments of the reaction solutions at 1h, 2h, and 3h (negative charge scan mode, m/z 400 - 2500).

negative charge scan mode (1h)		
Possible molecular fragments	Formula weight	The main spectral peak
$[Cu_3(OH)_3(SO_4)_2(H_2O)_3]^-$	487.84	487.3
$[Cu_3(OH)_3(SO_4)_2(H_2O)_6]^-$	540.5	540.2
$[Cu_3(OH)(SO_4)_3(H_2O)_4(CH_3OH)]^-$	599.95	600.40
$[Cu_3(OH)_4(pempH)(SO_4)(H_2O)_8]^-$	713.05	713.48
$[Cu_3(OH)(pempH)_2(SO_4)_2]^-$	827.5	827.57
$[Cu_6(OH)_5(pempH)_2(SO_4)_3(H_2O)_3]^-$	1237.42	1237.31
$[NaCu_6(OH)_4(pempH)_2(SO_4)_4(H_2O)_8(CH_3OH)]^-$	1460.62	1459.37
$[Cu_9(OH)_6(pempH)_3(SO_4)_5(H_2O)_2]^-$	1832.89	1831.47
$[Cu_{12}(OH)_4(pempH)(SO_4)_{10}(H_2O)(CH_3OH)]^-$	2054.78	2054.51
$[Cu_{11}(OH)_{11}(pempH)_4(SO_4)_4]^-$	2127.12	2127.54
$[Cu_{11}(OH)_6(pempH)_3(SO_4)_7(H_2O)_5]^-$	2204.14	2203.55
negative charge scan mode (2h)		
$[Cu_3(OH)_3(SO_4)_2(H_2O)_3]^-$	487.84	487.3
$[Cu_3(OH)_4(pempH)(SO_4)(H_2O)_8]^-$	713.05	713.48
$[NaCu_6(OH)_4(pempH)_2(SO_4)_4(H_2O)_8(CH_3OH)]^-$	1460.62	1459.37
$[Cu_9(OH)_6(pempH)_3(SO_4)_5(H_2O)_2]^-$	1832.89	1831.47
negative charge scan mode (3h)		
$[Cu_3(OH)_4(pempH)(SO_4)(H_2O)_8]^-$	713.05	713.48
$[NaCu_6(OH)_4(pempH)_2(SO_4)_4(H_2O)_8(CH_3OH)]^-$	1460.62	1459.37
$[Cu_9(OH)_6(pempH)_3(SO_4)_5(H_2O)_2]^-$	1832.89	1831.47
$Cu_{12}(OH)_{11}(SO_4)_5(pempH)_4(H_2O)_3(CH_3OH)_2]^-$	2404.27	2403.77

Table S6 Some recent reports on Cu-based coordination compounds for photothermal effect.

Compounds	Light source	Sample status	Maximum temperature	Stability	Reference
1	808 nm laser 1 W/cm^2	solid	49 °C (5min)	recyclable	This work
2			54 °C		
$[Cu_2(X9A)_4(CH_3CN)_2]$	Xenon lamp 300 mW	solid	28 °C (5min)	-	*Inorg. Chim. Acta,* 2021, **526**, 120531.
$\{[Cu_2(X9A)(dppm)_2(CH_3CN)](BF_4)\cdot(CH_3CN)\}$			27 °C (20min)	-	
$\{[Cu_2(X9A)_3(bpy)_2](BF_4)\cdot 0.5(H_2O)\}_2$			32 °C (20min)	-	
$[Cu_4(bpy)_4(1\text{-}NTAA)_5](BF_4)_3\cdot 3(CH_3OH)\cdot H_2O$	Xenon lamp 300 mW	solid	40 °C (15min)	-	*Inorg. Chim. Acta,* 2020, **508**, 119608.
$[Cu_2(1\text{-}NTAA)_4(CH_3CN)_2]\cdot 2(CH_3CN)$			37 °C (10min)	-	
$\{[Cu_2(2\text{-}NTA)_4(CH_3CN)_2]\cdot 2.5(CH_3CN)\}$			36 °C (10min)	-	
HKUST-1 $[Cu_3(BTC)_2(H_2O)_3]$	808 nm 0.8 W/cm^2	500μg/mL in PBS	35 °C (20min)	recyclable	*J. Hazard. Mater.* 2020, **390**, 122126.
Cu-BTC $[(Cu_3(C_9H_3O_6)_2]$	808 nm 1 W/cm^2	80 μg/mL in PBS	34 °C (10 min)	-	*Acta Biomater.* 2023, **158**, 660.
Cu-dhba $[Cu_3(dhba)_2(OH)_2(H_2O)_4]$	808 nm 0.288 W/cm^2	solid	115 °C (within seconds)	recyclable	*Cryst. Growth Des.* 2023, **23**, 2, 1211.
CuNRs Cu-nanorods	980 nm 1.2 W/cm^2	disperse in water	60 °C (5min)	recyclable	*Angew. Chem. Int. Ed.* 2019, **58**, 9275 – 9281
Cu-TCPP Cu tetra-(4-carboxyphenyl) porphyrin	Xenon lamp	film	120 °C (3 min)	recyclable	*Nat. Commun.* 2024, **15**, 2125
Cu-POM Cu-doped polyoxometalate clusters	808 nm 1 W/cm^2	solution	50 °C (3 min)	recyclable	*Adv. Mater.* 2023, **35**, 2303432

Cu-PCy JNPs Cu-porphyrin cyanine dye nanoparticles	808 nm 1 W/cm^2	solution	56.6 °C (10 min)	recyclable	*Angew. Chem. Int. Ed.* 2024, e202404395
[Cu_2(DNB-Cl)$_4$(H_2O)$_2$]·2H_2O 3,5-dinitro-4-chlorobenzoic acid (HDNB-Cl)	808 nm 1 W/cm^2	solid	130.6 °C (5min)	recyclable	*CrystEngComm,* 2022, **24**, 7493–7499
[Cu_2(DNB-Cl)$_3$(OH)(H_2O)$_2$]·H_2O 3,5-dinitro-4-chlorobenzoic acid (HDNB-Cl)			114.8 °C (5min)		
[Cu_2(DNB-O)(OH)$_2$(H_2O)$_2$] 3,5-dinitro-4-hydroxybenzoic acid (HDNB-OH)			110.5 °C (5min)		
Cu-THQNPs [Cu($C_{14}H_8O_6$)]$_n$	808 nm 1 W/cm^2	solution	52.1 °C (5min)	recyclable	*ACS Appl. Mater. Interfaces* 2018, **10**, 25203.

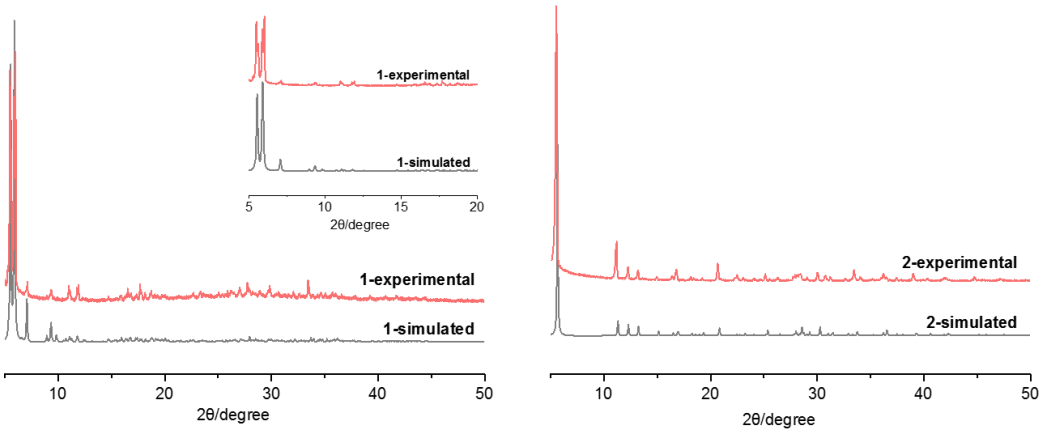

Figure S1. PXRD patterns of simulated from the single-crystal data of **1** and **2** (black), as-synthesized **1** and **2** (red).

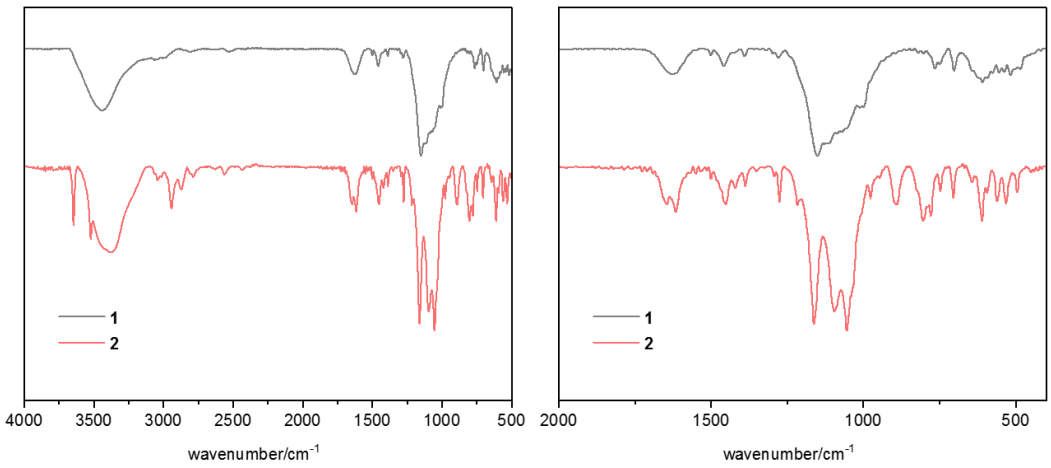

Figure S2. The IR spectra of compounds **1** and **2**.

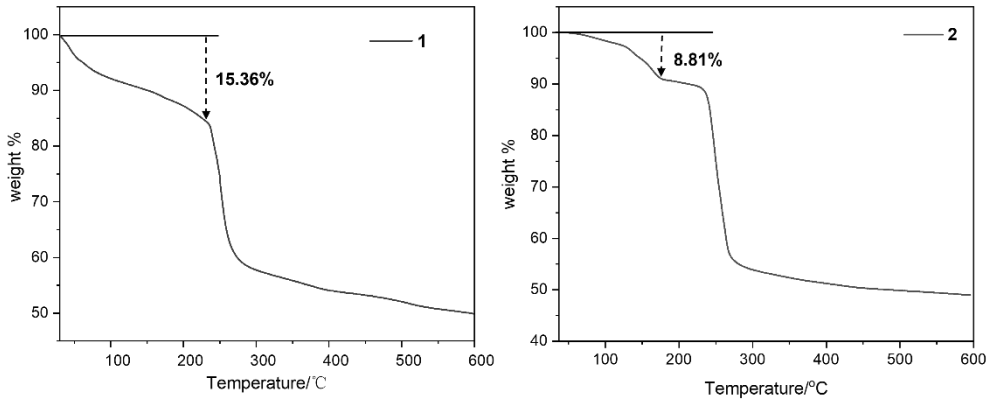

Figure S3. TGA curves of **1** and **2**. TGA curves of **1** and **2**. The weight loss in the ranges of 30-230 °C is 15.36% for **1**, agreeing with the release of 45.5 water molecules (35 lattice water molecules and 10.5 coordinated water molecules, calc. 15.28 %). The weight loss in the ranges of 50-175°C is 8.81% for **2**, agreeing with the release of 1.5 water molecules (0.5 lattice water molecule and 1 coordinated water molecule) and 0.5 methanol molecule (calc. 8.6%).

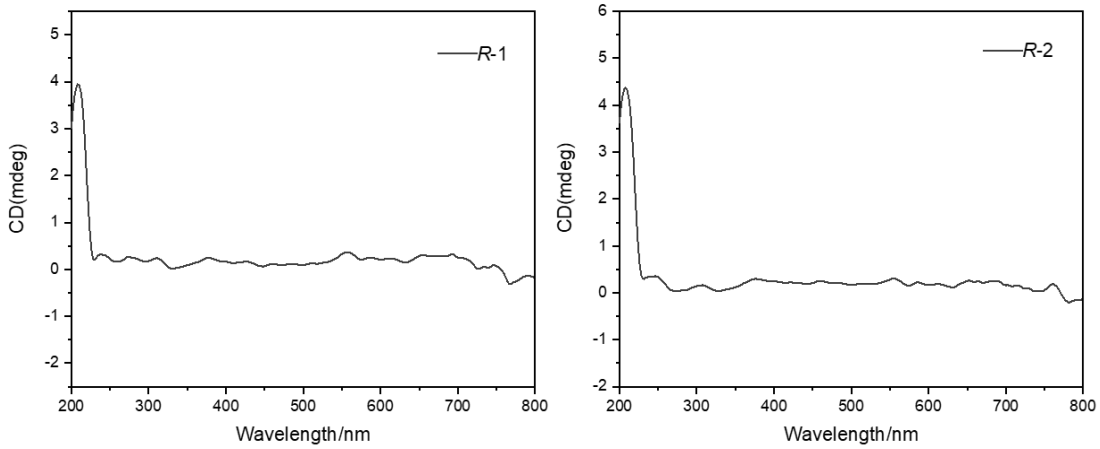

Figure S4. The solid state CD spectra of ***R*-1** and ***R*-2**.

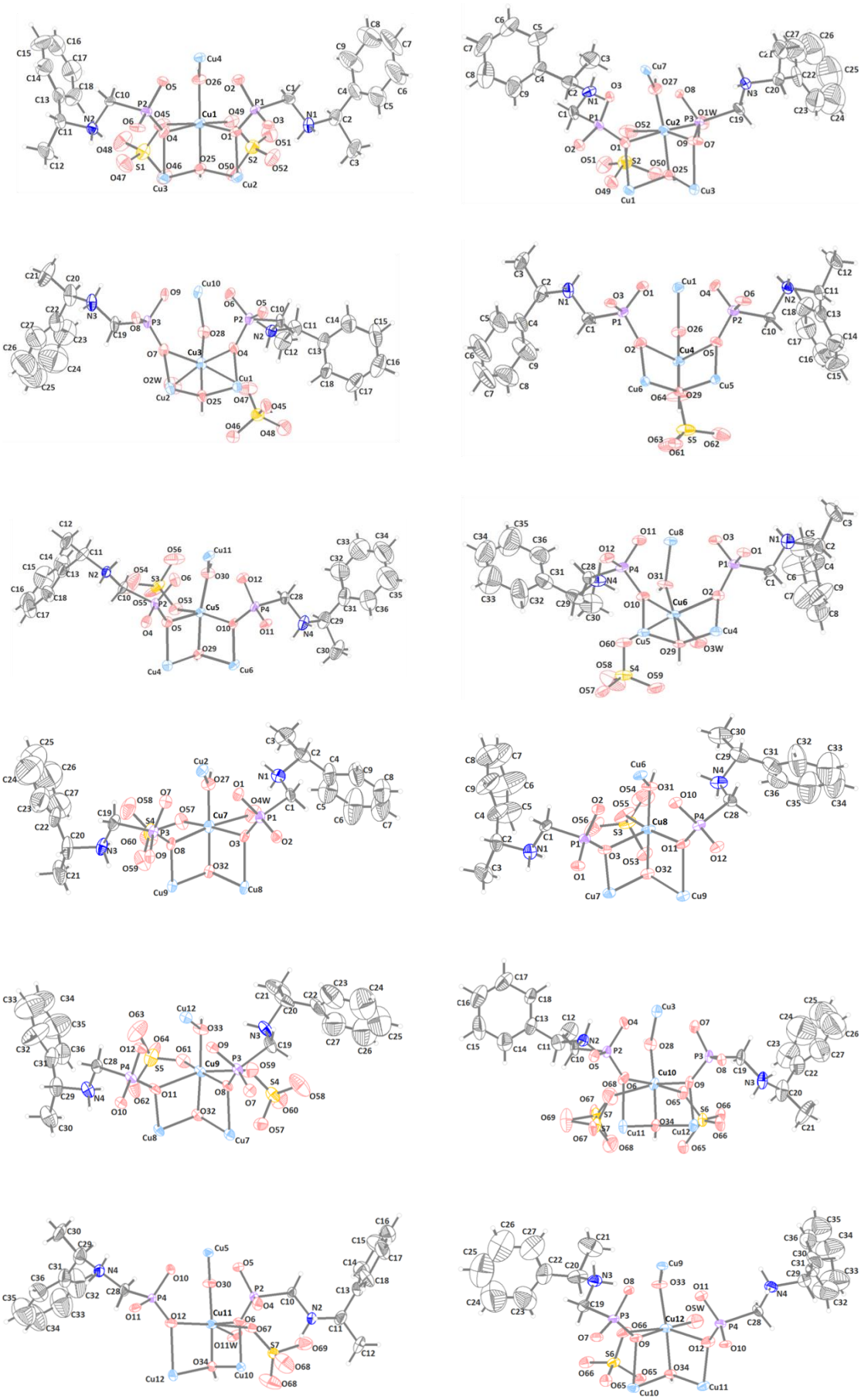

Figure S5. The coordination environment of Cu1 to Cu12 in Cu_{12}-A.

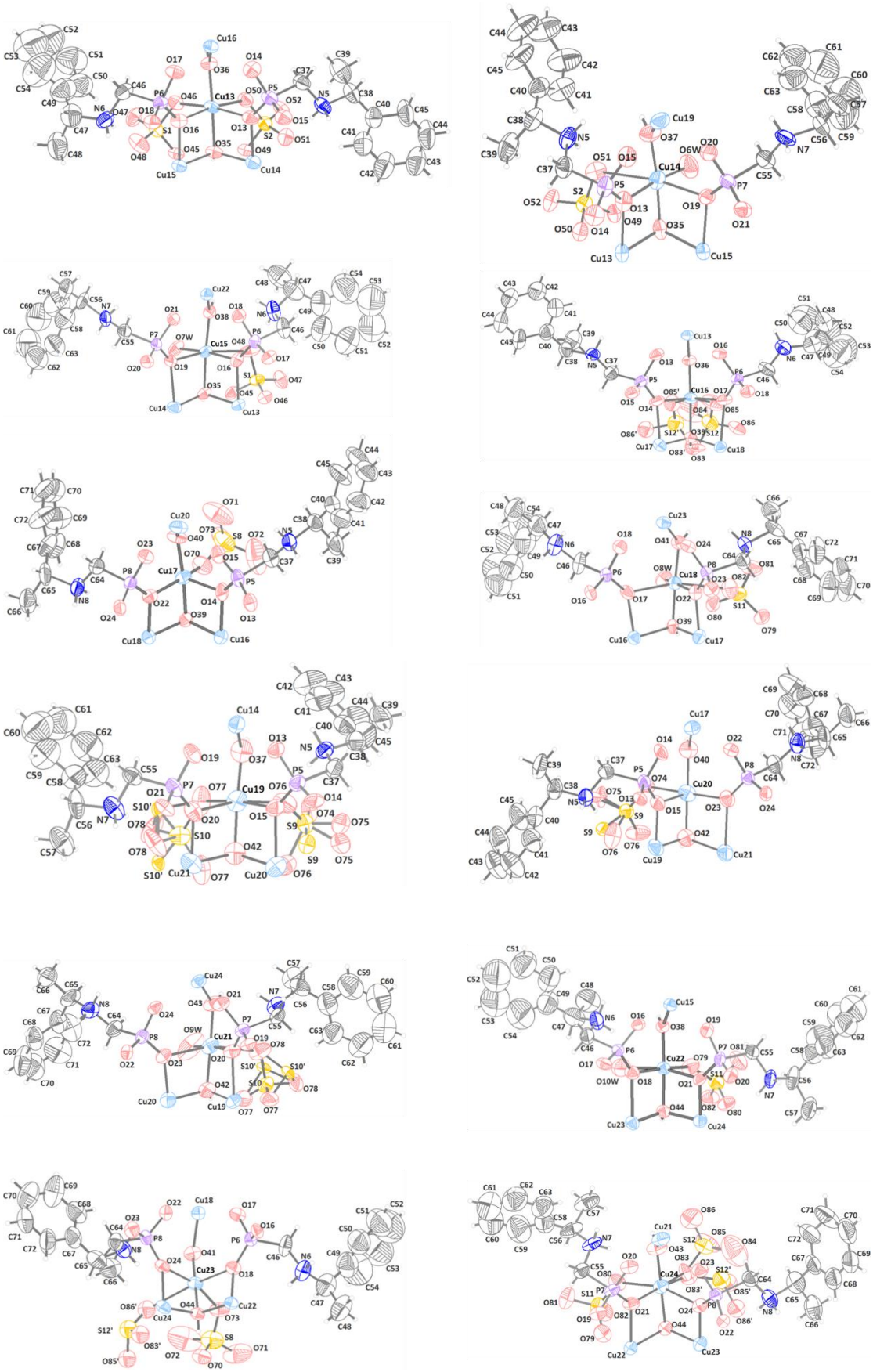

Figure S6. The coordination environment of Cu12 to Cu24 in Cu_{12}-B.

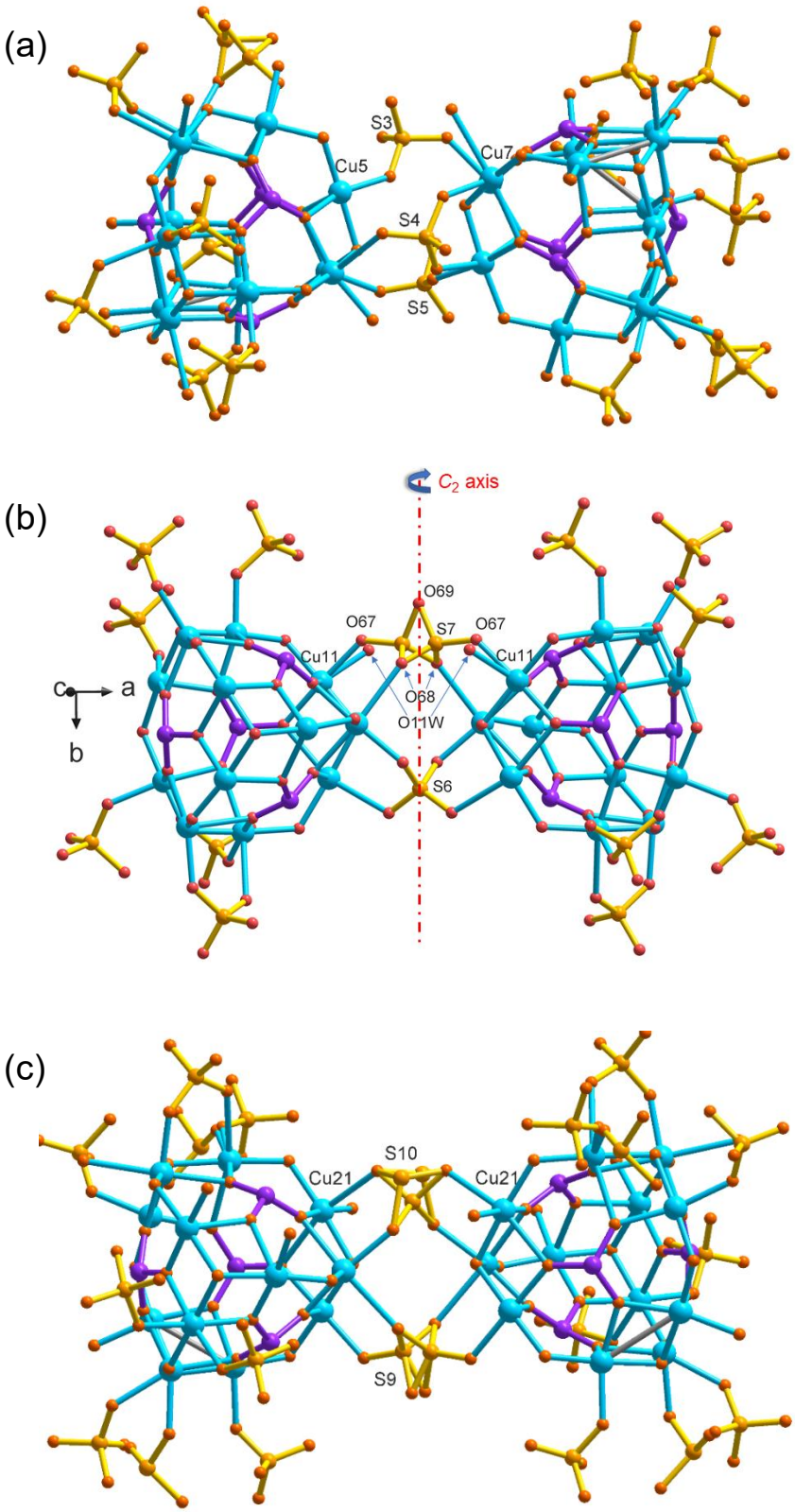

Figure S7. (a) Adjacent Cu_{12}-A clusters connected by three sulfate bridges (S3, S4, S5). (b) Adjacent Cu_{12}-A clusters connected by two sulfate bridges (S6 and S7) located at the C_2 axis. (c) Adjacent Cu_{12}-B clusters connected by two sulfate bridges (S9 and S10) located at the C_2 axis in compound **1**.

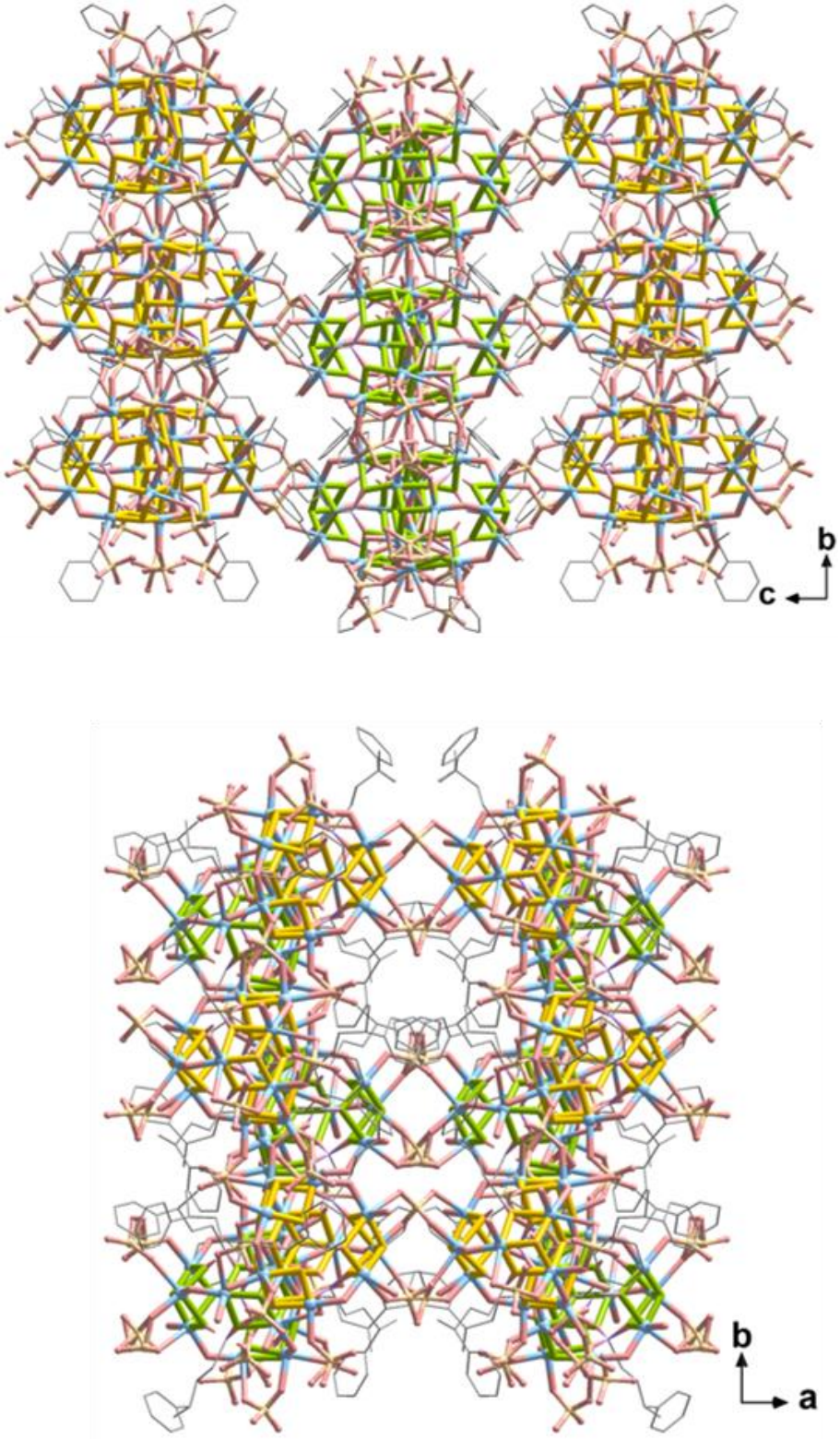

Figure S8. The 3D framework of **1** along *bc* plane and *ab* plane.

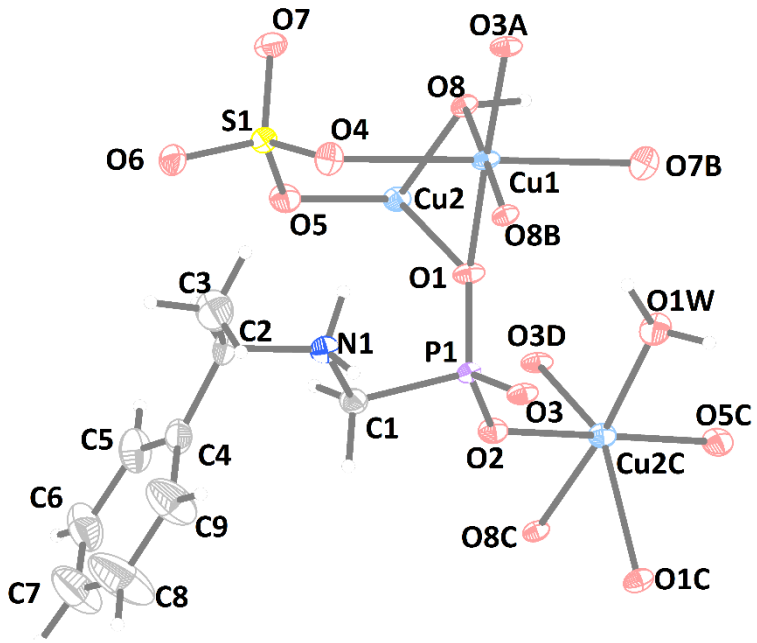

Figure S9. The asymmetric unit of **2**.

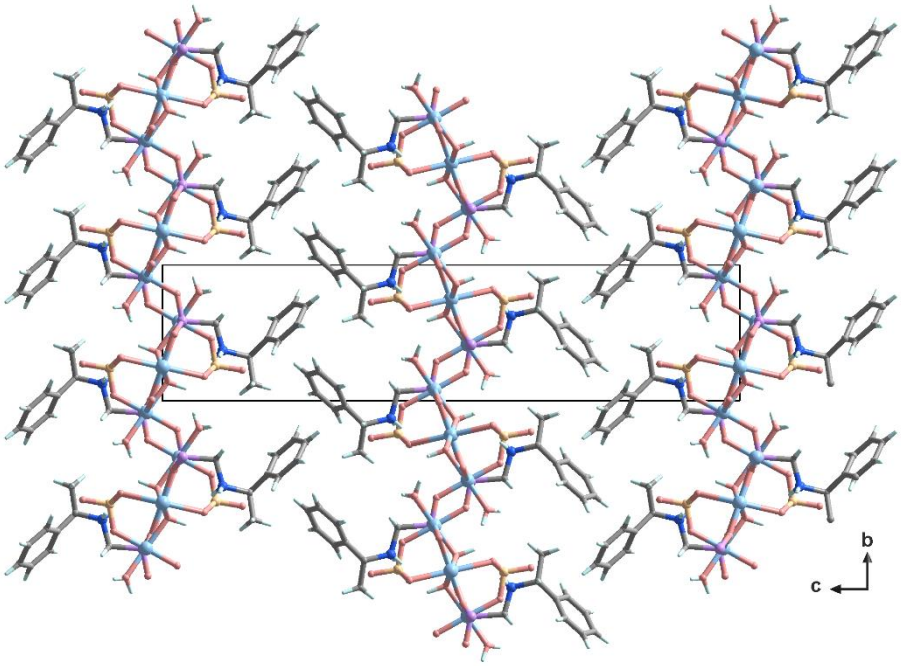

Figure S10. The 3D packing structure of **2** viewed along the *a*-axis.

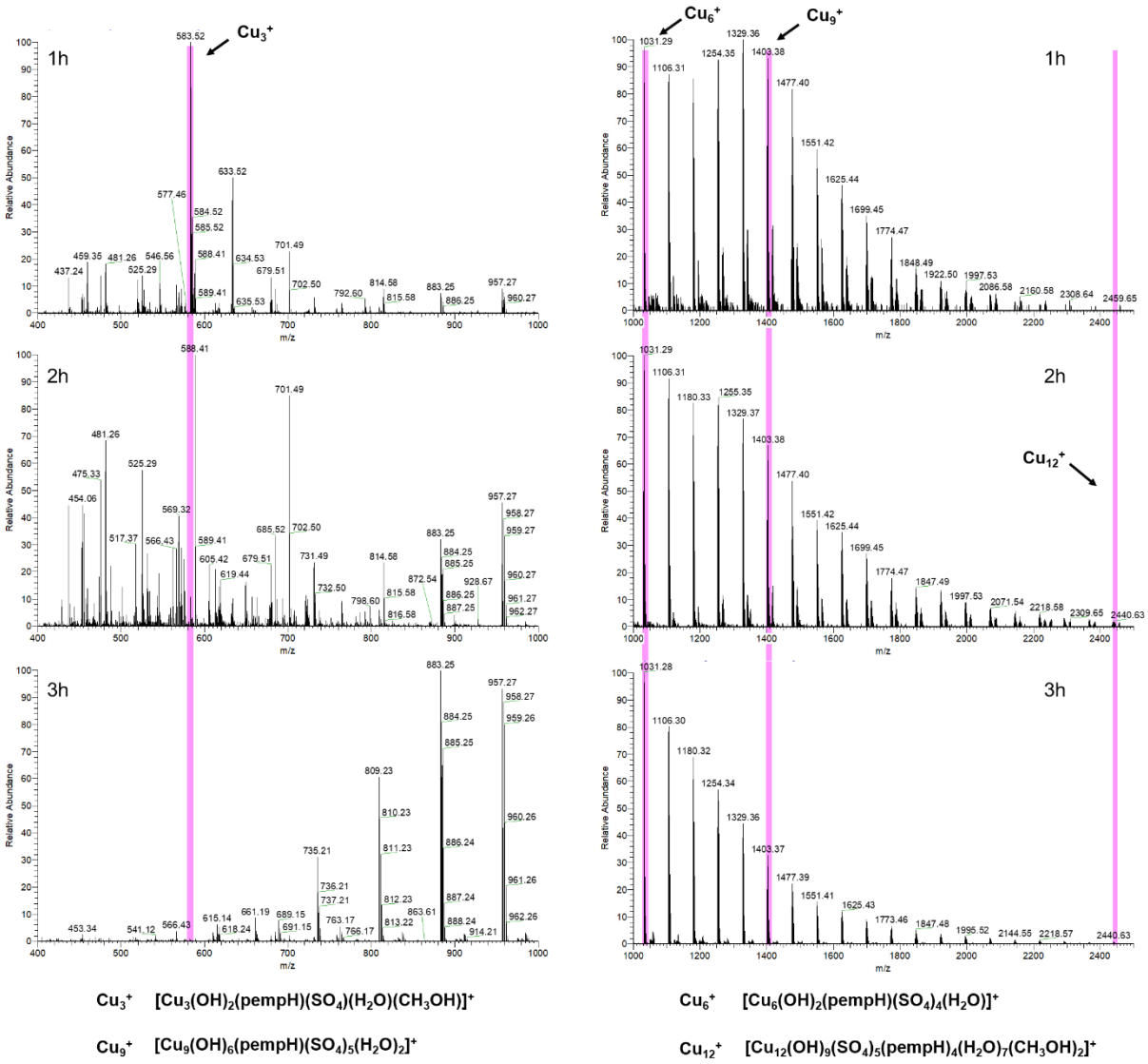

Figure S11. Time-dependent ESI-MS of the reaction solutions at 1h, 2h, and 3h (positive charge scan mode, m/z 400 - 2500).

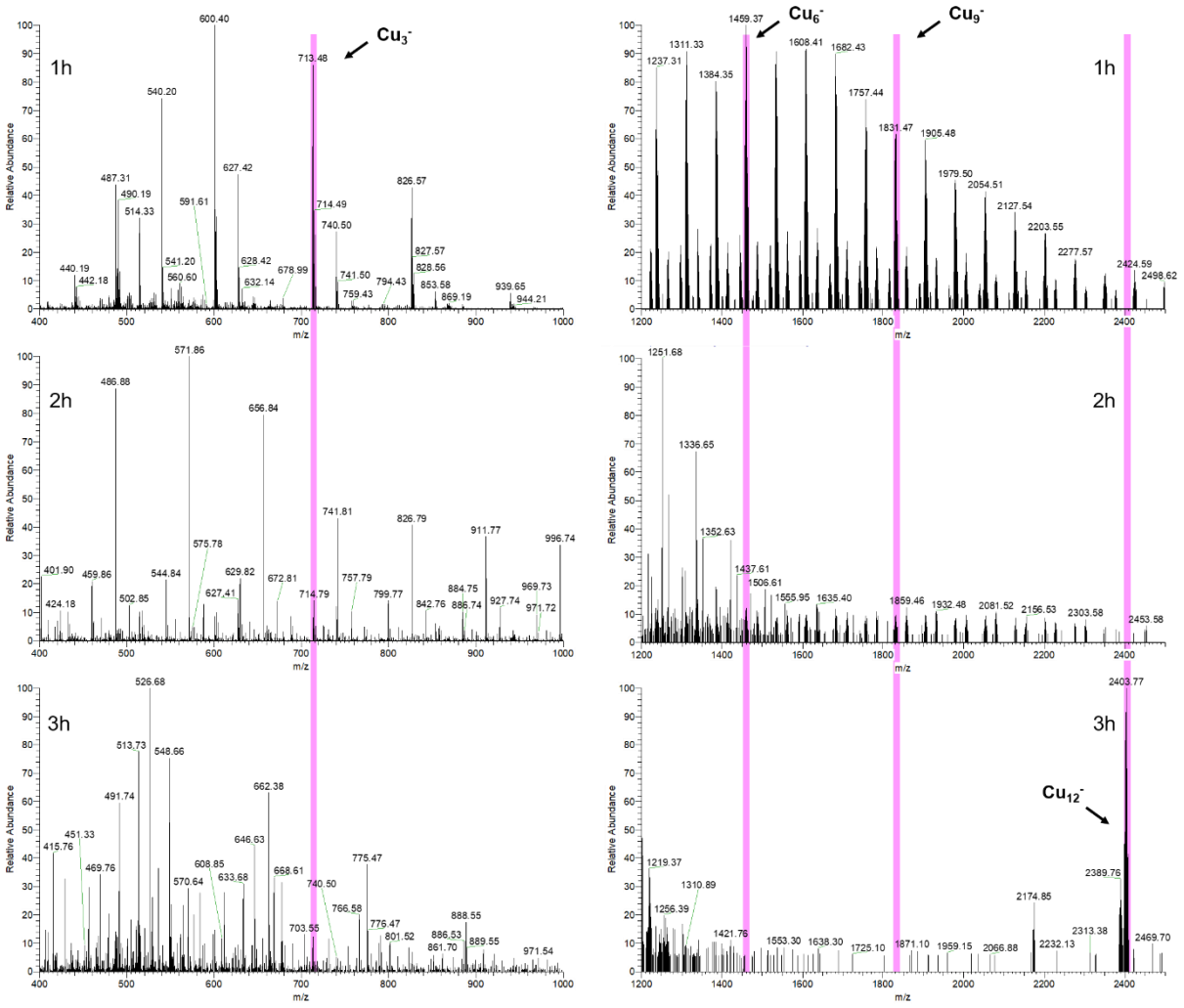

Cu_3^- $[Cu_3(OH)_4(pempH)(SO_4)(H_2O)_8]^-$

Cu_6^- $[NaCu_6(OH)_4(pempH)_2(SO_4)_4(H_2O)_8(CH_3OH)]^-$

Cu_9^- $[Cu_9(OH)_6(pempH)_3(SO_4)_5(H_2O)_2]^-$

Cu_{12}^- $[Cu_{12}(OH)_{11}(SO_4)_5(pempH)_4(H_2O)_3(CH_3OH)_2]^-$

Figure S12. Time-dependent ESI-MS of the reaction solutions at 1h, 2h, and 3h (negative charge scan mode, m/z 400 - 2500).

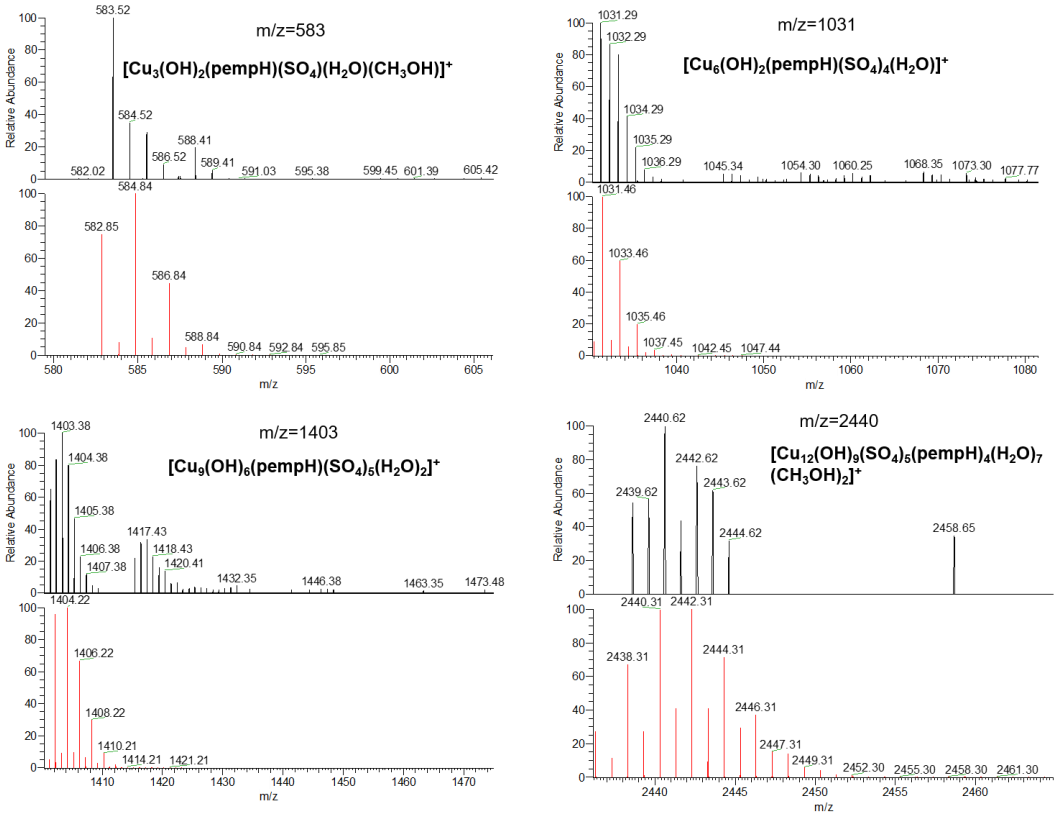

Figure S13. Comparison of the calculated (red) and experimental (black) isotope distribution patterns of each proposed species (positive charge scan mode).

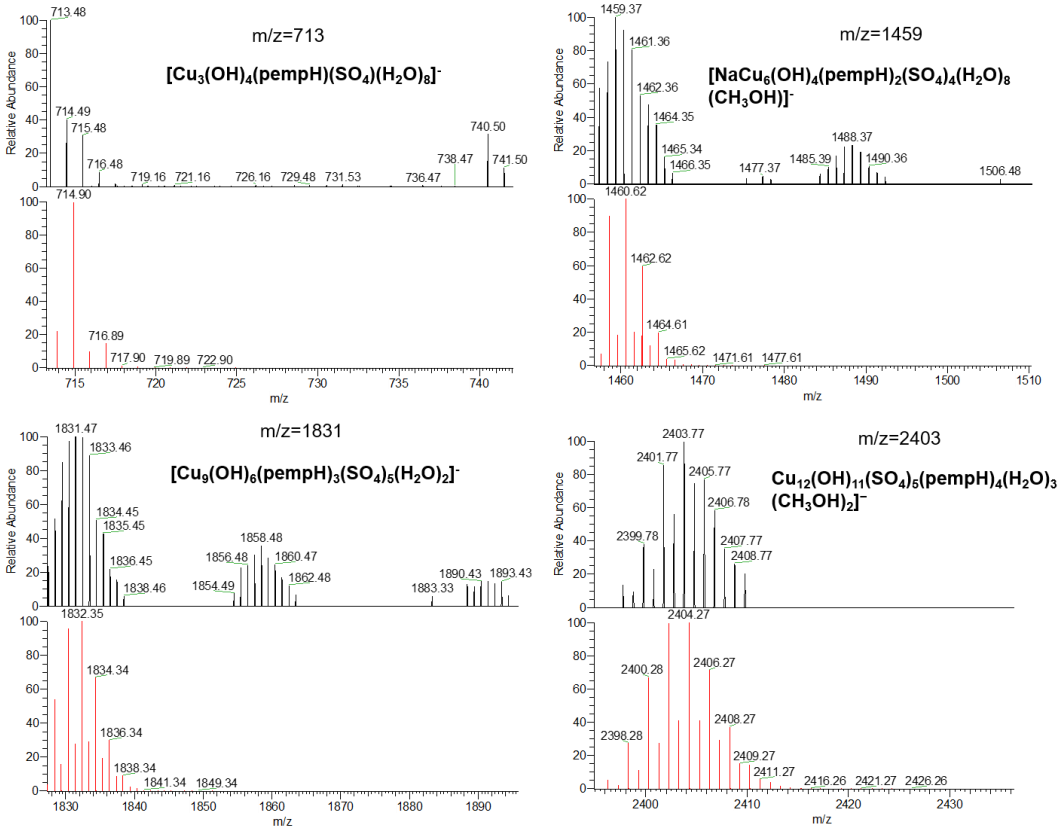

Figure S14. Comparison of the calculated (red) and experimental (black) isotope distribution patterns of each proposed species (negative charge scan mode).

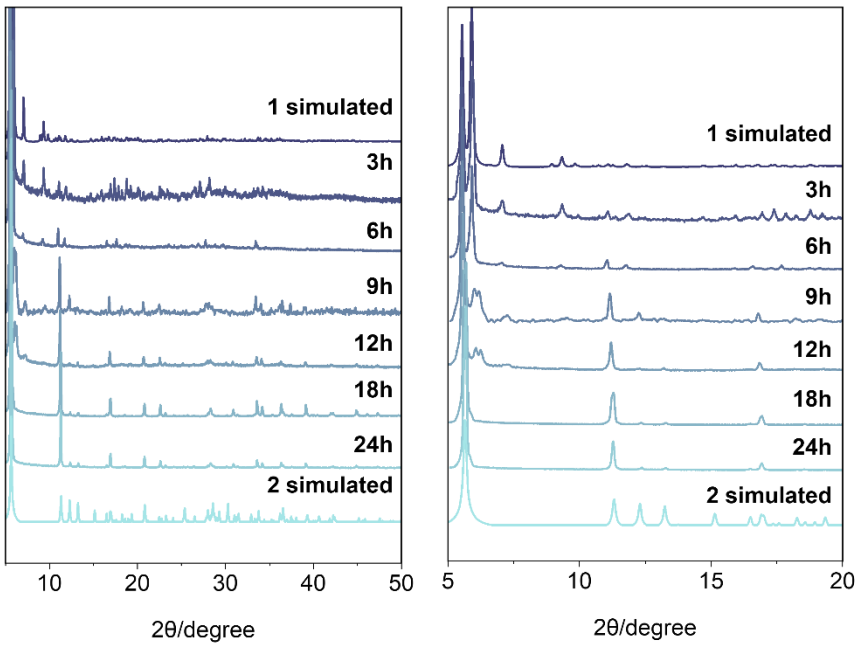

Figure S15. The PXRD spectra of the reaction products from **1** to **2** for different periods of time after solvothermal reactions of $CuSO_4 \cdot 5H_2O$ and *R*-pempH$_2$ at 90°C, when metal:ligand molar ratio was 6:1.

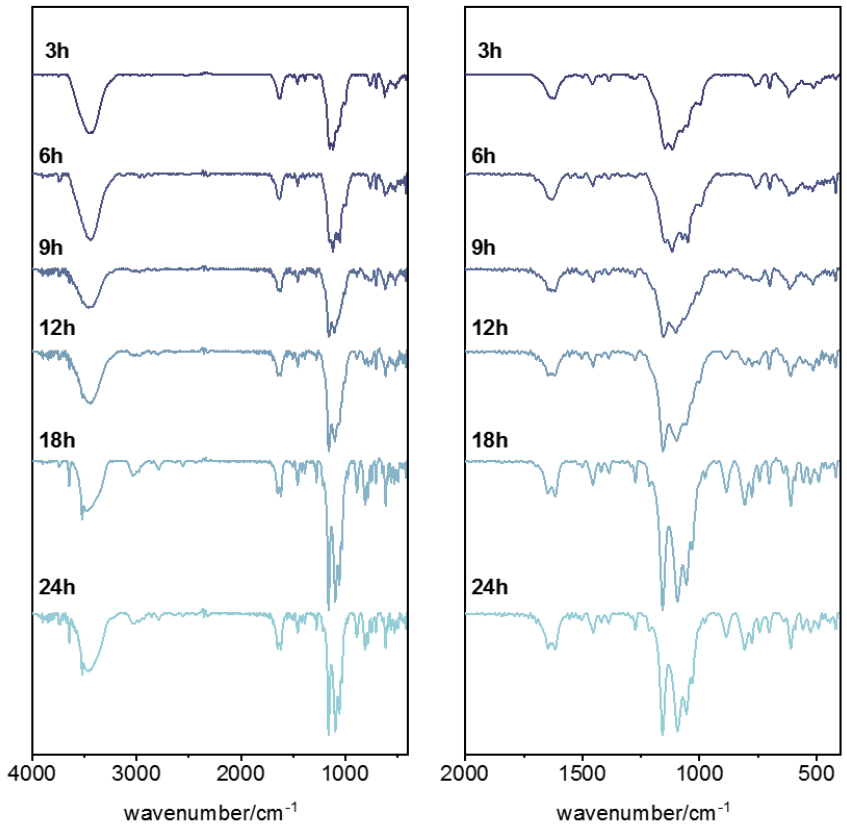

Figure S16. The IR spectra of the reaction products from **1** to **2** for different periods of time after solvothermal reactions of $CuSO_4 \cdot 5H_2O$ and *R*-pempH$_2$ at 90°C, when metal:ligand molar ratio was 6:1 (Left: 4000-400 cm^{-1}, Right: 2000-400 cm^{-1}).

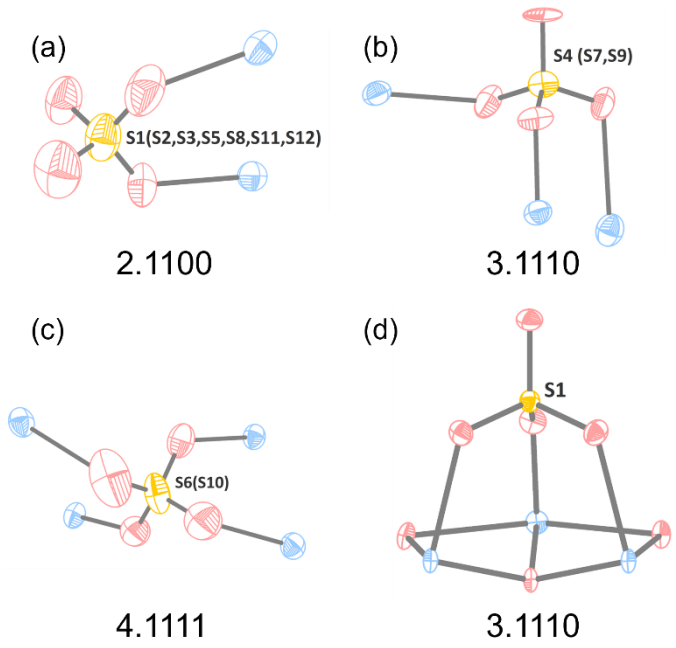

Figure S17. The coordination modes of the sulfato ligand of **1** (a,b,c) and **2** (d).

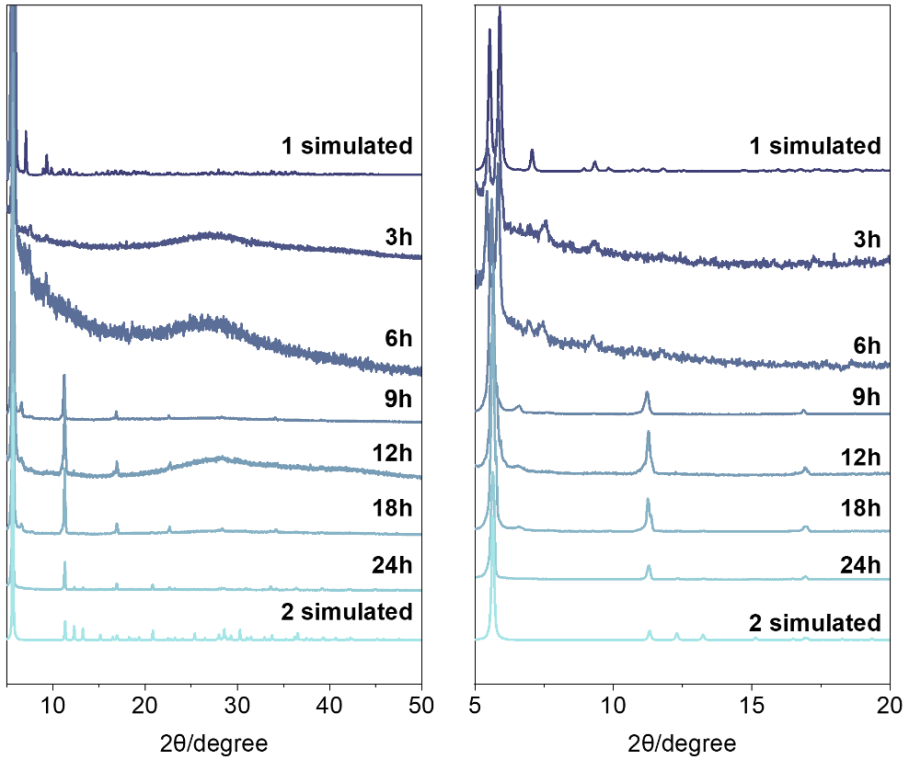

Figure S18. The PXRD spectra of the reaction products from **1** to **2** for different periods of time after solvothermal reactions of $CuSO_4 \cdot 5H_2O$ and *R*-pempH$_2$ at 90°C, when metal:ligand molar ratio was 4:1.

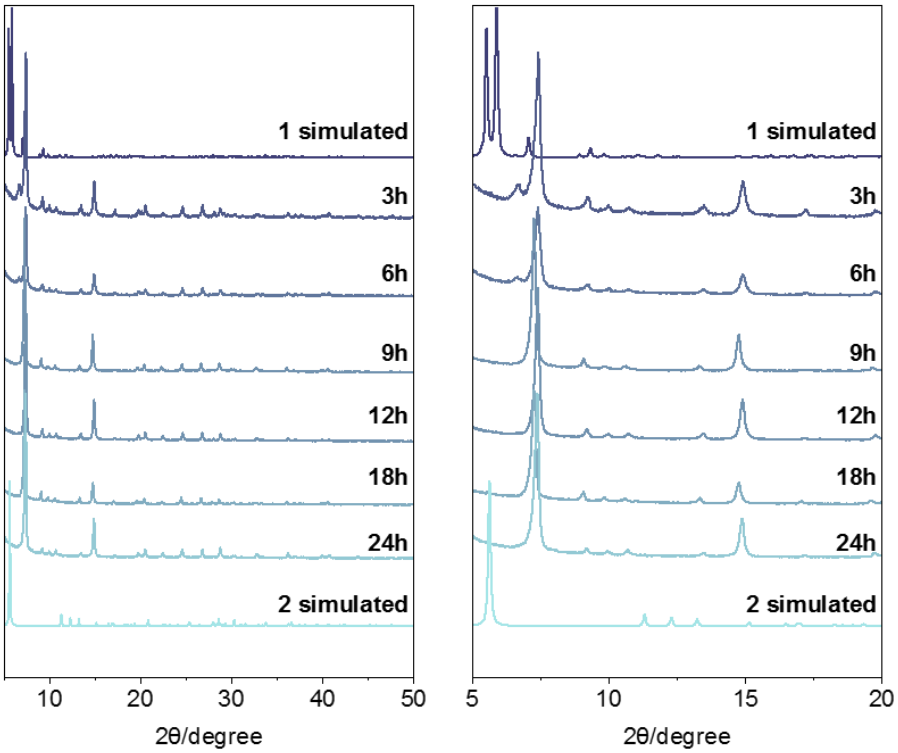

Figure S19. The PXRD spectra of the reaction products for different periods of time after solvothermal reactions of $CuSO_4 \cdot 5H_2O$ and *R*-pempH$_2$ at 90°C, when metal:ligand molar ratio was 3:1.

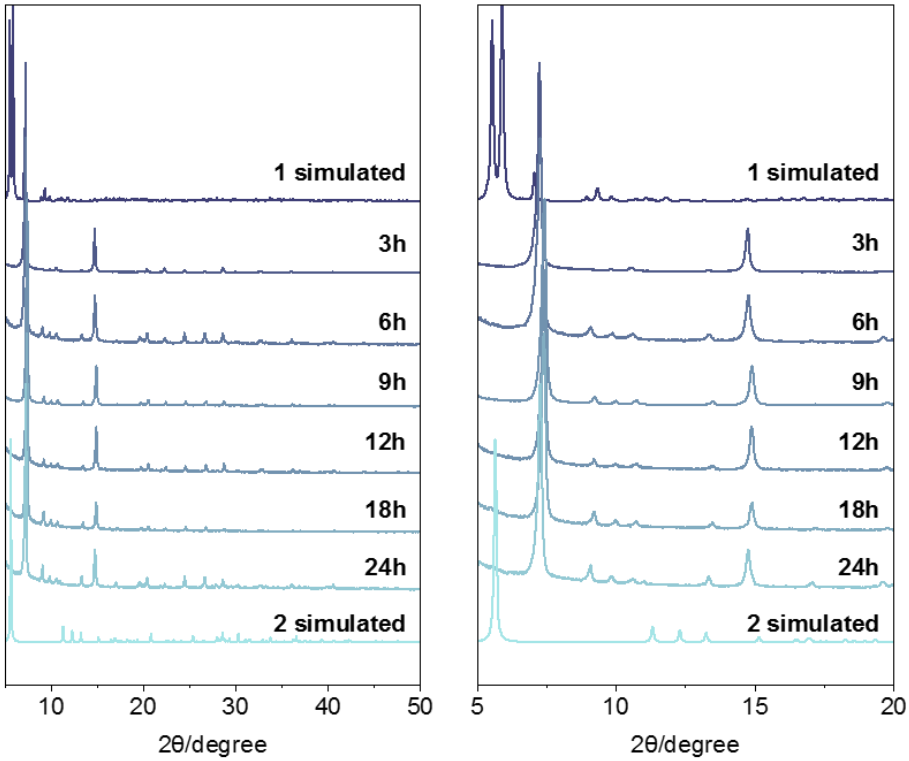

Figure S20. The PXRD spectra of the reaction products for different periods of time after solvothermal reactions of $CuSO_4 \cdot 5H_2O$ and *R*-pempH$_2$ at 90°C, when metal:ligand molar ratio was 2:1.

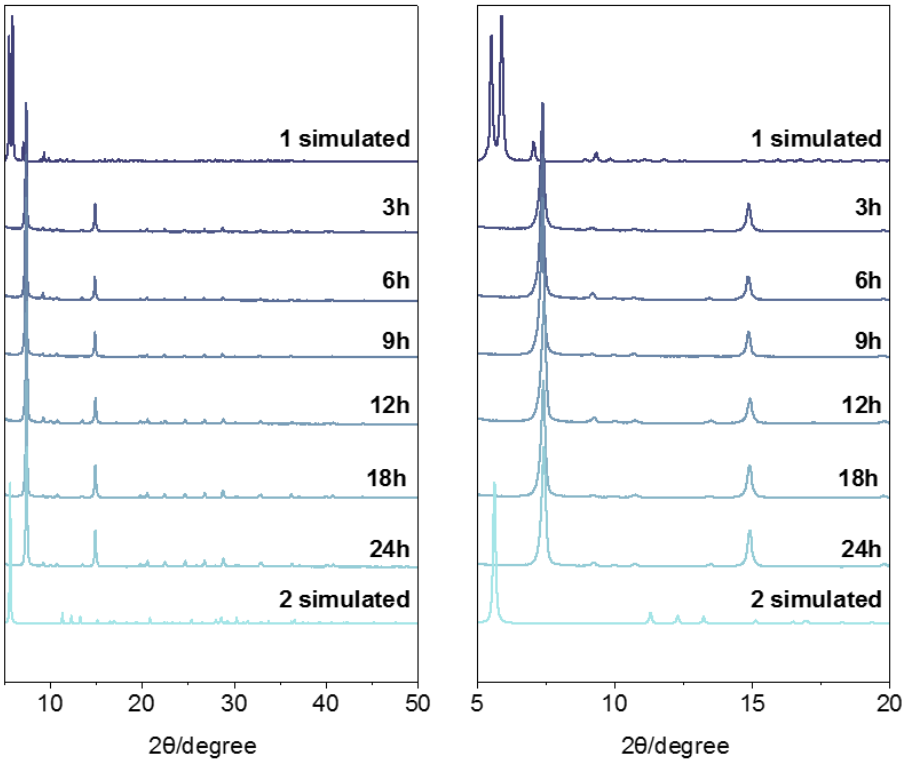

Figure S21. The PXRD spectra of the reaction products for different periods of time after solvothermal reactions of $CuSO_4 \cdot 5H_2O$ and *R*-pempH$_2$ at 90°C, when metal:ligand molar ratio was 1:1.

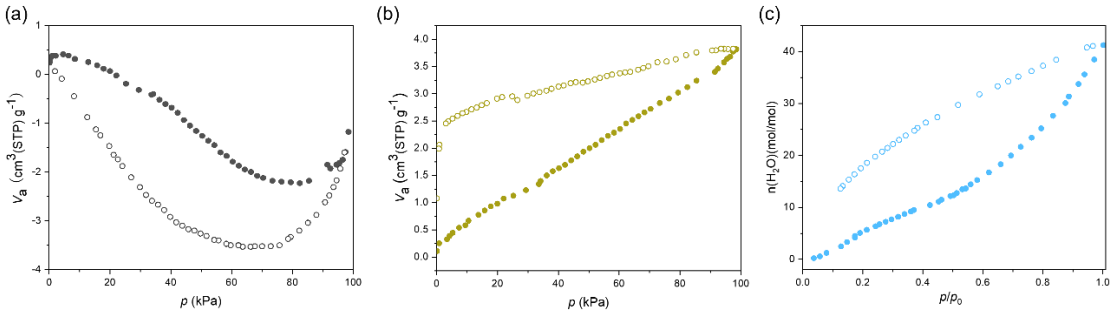

Figure S22. (a) The N_2 adsorption (filled) and desorption (open) isotherms from 0 to 100 kPa at 77K for compound **1**; (b) the CO_2 adsorption (filled) and desorption (open) isotherms from 0 to 100 kPa at 195K for compound **1**; (c) water adsorption (filled) and desorption (open) isotherms at 298 K for compound **1**.

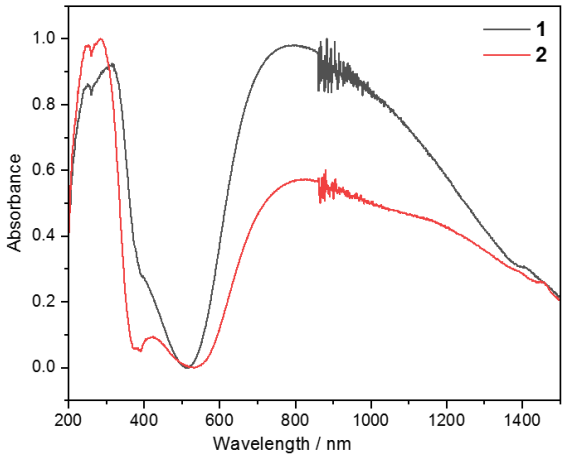

Figure S23. The solid state UV-vis spectra of **1** and **2**.

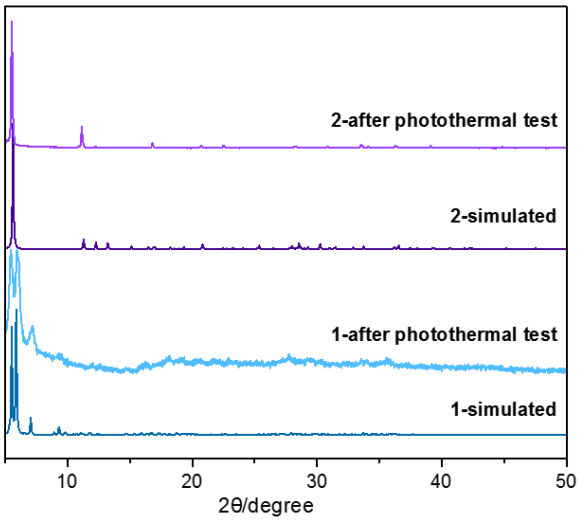

Figure S24. PXRD patterns of **1** and **2** after photothermal testing. The simulated patterns of **1** and **2** are given for comparison.